

Low temperature magnetism in the perovskite substrate DyScO₃

X. Ke, C. Adamo, D. G. Schlom, M. Bernhagen, R. Uecker, and P. Schiffer

Citation: *Applied Physics Letters* **94**, 152503 (2009); doi: 10.1063/1.3117190

View online: <http://dx.doi.org/10.1063/1.3117190>

View Table of Contents: <http://scitation.aip.org/content/aip/journal/apl/94/15?ver=pdfcov>

Published by the *AIP Publishing*

Articles you may be interested in

[Magnetic and transport properties of epitaxial stepped Fe₃O₄\(100\) thin films](#)

Appl. Phys. Lett. **105**, 132408 (2014); 10.1063/1.4897001

[Temperature and concentration dependent magnetic properties of epitaxial Fe_{1-x}Cr_x-alloy films in the high Cr-concentration regime](#)

J. Appl. Phys. **116**, 033906 (2014); 10.1063/1.4890233

[Magnetic properties of room temperature grown epitaxial Co_{1-x}Ru_x-alloy films](#)

Appl. Phys. Lett. **103**, 102410 (2013); 10.1063/1.4820189

[Structure, magnetic, and microwave properties of thick Ba-hexaferrite films epitaxially grown on GaN / Al₂O₃ substrates](#)

Appl. Phys. Lett. **96**, 242502 (2010); 10.1063/1.3446867

[Magnetic properties of DyAs and DyP \(001\) films](#)

J. Appl. Phys. **85**, 4970 (1999); 10.1063/1.370061

You don't still use this cell phone

or this computer

Why are you still using an AFM designed in the 80's?

It is time to upgrade your AFM

Minimum \$20,000 trade-in discount for purchases before August 31st

Asylum Research is today's technology leader in AFM

dropmyoldAFM@oxinst.com

OXFORD
INSTRUMENTS
The Business of Science®

Low temperature magnetism in the perovskite substrate DyScO₃

X. Ke,¹ C. Adamo,² D. G. Schlom,² M. Bernhagen,³ R. Uecker,³ and P. Schiffer^{1,a)}

¹Department of Physics and Materials Research Institute, Pennsylvania State University, University Park, Pennsylvania 16802, USA

²Department of Materials Science and Engineering, Pennsylvania State University, University Park, Pennsylvania 16802-5005, USA

³Institute for Crystal Growth, Max-Born-Street 2, D-12489 Berlin, Germany

(Received 3 January 2009; accepted 20 March 2009; published online 14 April 2009)

We investigate the low temperature magnetic properties of crystalline DyScO₃, a material that has seen increasing importance as a substrate for the growth of strained perovskite films. The compound exhibits strong magnetic anisotropy with an easy axis along the [100] direction and a hard axis along the [001] direction, respectively, attributable to magnetocrystalline anisotropy. We find that DyScO₃ undergoes a magnetic phase transition at 3.1 K, presumably from paramagnetism to antiferromagnetic long range order. The presence of such a transition and the magnetic anisotropy suggests the possibility of significant substrate impact on studies of the magnetism of the epitaxial thin films grown on this material. © 2009 American Institute of Physics. [DOI: 10.1063/1.3117190]

Over the past five years, rare-earth perovskite scandates with different lattice parameters¹ have been exploited to strain-engineer epitaxial ferroelectric and multiferroic perovskite thin films. The biaxial strain due to lattice mismatch can dramatically alter the properties of commensurate epitaxial films.² For instance, enhanced ferroelectricity with larger polarization and higher paraelectric-to-ferroelectric transition temperature has been achieved in compressively strained BaTiO₃ thin films grown on DyScO₃ and GdScO₃ substrates.³ Tensile strained SrTiO₃ films, grown on DyScO₃ substrates, exhibit ferroelectric behavior at room temperature compared with the paraelectric behavior of bulk unstrained SrTiO₃.⁴ Epitaxial strain can also significantly affect phase transitions and the magnetic anisotropy of magnetic oxide thin films grown on top of these rare-earth scandates.⁵

In addition to serving as substrates for epitaxial thin film growth, rare-earth perovskite scandates are of interest for their intrinsic properties. For the rare earths Ho–La, they are all isostructural with the orthorhombic GeFeO₃ perovskite structure with *Pbnm* space group.¹ Smaller rare earths, e.g., all the way down to Lu, can form rare-earth scandates with the same perovskite structure using epitaxial stabilization.⁶ The thermal expansion coefficients of bulk rare-earth scandates are similar to other oxide perovskites.^{7,8} Interest in their potential application has been motivated by large band gaps,^{9,10} high dielectric constants,¹¹ and the ability to grow epitaxial rare-earth scandate thin films on Si substrates.¹² The magnetic properties of these materials, which may be important especially when they are used as substrates for magnetic oxide thin films, have not been reported in detail,¹³ although in Ref. 13 the inverse susceptibility of gadolinium scandate powder (GdScO₃) shows a negative value of Curie–Weiss temperature. In this paper, we report the magnetic properties of single crystal DyScO₃ at low temperatures. We find a strong magnetic anisotropy with an easy axis along the [100] direction and a hard axis along the [001] direction respectively—attributable to magnetocrystalline anisotropy. We also observe a phase transition to long range antiferro-

magnetic ordering at $T_N \sim 3.1$ K. Both of these findings result in important considerations for the study of thin films grown on this substrate.

The growth of the DyScO₃ single crystals used in this study is reported elsewhere.⁸ In the convention of the *Pbnm* space group, the orthorhombic unit cell structure of DyScO₃ has lattice constants $a = 5.440 \pm 0.001$ Å, $b = 5.717 \pm 0.001$ Å, and $c = 7.903 \pm 0.001$ Å at room temperature.¹⁴ DyScO₃ has an orthorhombically distorted perovskite structure because its Goldschmidt tolerance factor is significantly less than 1 (Ref. 15) and it is often referred to as pseudocubic with a lattice constant of about 3.944 Å.⁷ The samples measured in this study are (110)-oriented plates with in-plane edges along the $[\bar{1}10]$ and [001] directions. Note that the indices used in this study are referred to the orthorhombic unit cell. We measured the magnetization with a Quantum Design superconducting quantum interference device magnetometer, and the ac magnetic susceptibility with a Quantum Design PPMS with the ACMS option.

In the main panels of Fig. 1, we plot the temperature dependence of the dc susceptibility of DyScO₃ for the low temperature regime with a 100 Oe magnetic field applied along the [100], [010] [001], [110], and $[\bar{1}10]$ directions. Field-cooled (FC) and zero-field-cooled (ZFC) measurements were made on warming, and we found that the measured susceptibility is the same for both FC and ZFC samples within the uncertainty of our measurements. All the curves show a maximum of susceptibility around 3.1 K, although there is a strong anisotropy evident in the magnitude of the susceptibility. The sharp drop in the susceptibility, combined with the imperceptible difference between FC and ZFC curves, strongly suggests a phase transition to long range antiferromagnetic ordering at a Néel temperature of $T_N \sim 3.1$ K. The peak in the magnetization shifts to lower temperature with increasing fields (data not shown), which is a characteristic of an antiferromagnetic state and indicates its suppression due to the larger Zeeman interaction. Compared with the susceptibility measured along different crystalline directions, the largest and the smallest value of susceptibility with the field applied along the [100] and [001] directions,

^{a)}Electronic mail: schiffer@phys.psu.edu.

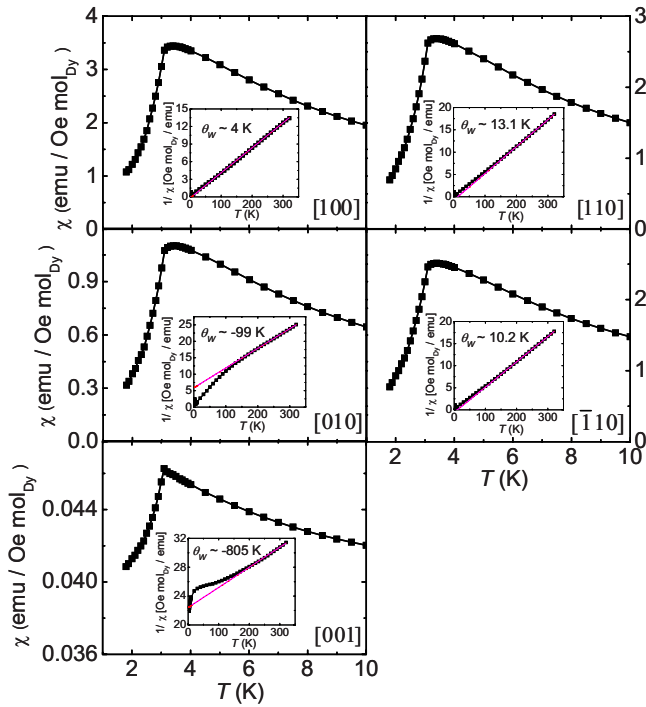


FIG. 1. (Color online) The temperature dependence of the dc susceptibility of DyScO_3 with a 100 Oe field applied along five different crystalline directions. Note the difference in the scale of the y-axes. The inverse susceptibility curves are shown in the inset figures. The pink lines represent the Curie-Weiss fit over the temperature range $T=200\text{--}320$ K.

respectively, suggest strong magnetic anisotropy with the easy axis of the antiferromagnetic order along the [100] direction and the [001] direction being the hard axis.

The insets in Fig. 1 show the inverse susceptibility, and the pink curves represent the Curie-Weiss fit over the temperature range $T=200\text{--}320$ K. We note that the shape of the inverse susceptibility curves are dramatically different for the measurement field applied along the [100], [010], and [001] directions, and the Weiss temperatures (θ_w) derived from the Curie-Weiss fits differ markedly along the [100] and [001] directions. Additionally, the values of the effective moment derived from the slope of the inverse susceptibility deviate significantly from that expected from the free ion. As mentioned above, DyScO_3 has an orthorhombic structure with the smaller lattice constant along the [100] direction and the longer axis along the [001] direction. We attribute the anisotropy to the effect of crystal fields on the ground state of Dy^{3+} ions, which is discussed in more detail below.

The observed strong magnetic anisotropy is also supported by isothermal magnetic measurements. Figure 2(a) shows the field dependence of magnetization M at $T=1.8$ K with the magnetic field applied along the aforementioned five crystallographic directions. We see that, with the exception of the [001] direction, M increases linearly at low fields followed by a steeper increase around 0.3 T and finally saturates at larger fields. This behavior is characteristic of a spin-flop transition, providing further support for the existence of an antiferromagnetic state at low temperature. The fact that the saturation field is smaller when the magnetic field is applied along the [100] direction than that along other directions, in combination with the comparison of saturation magnetization, suggests that the [100] direction is the easy axis, [001] is the hard axis, and the [010] is the intermediate

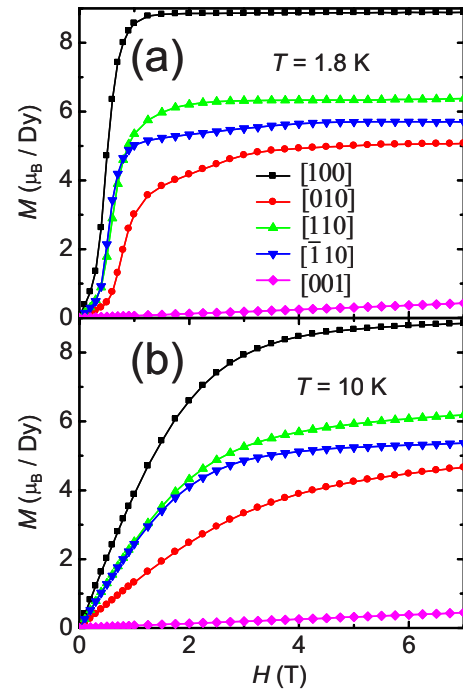


FIG. 2. (Color online) The field dependence of the magnetization at $T=1.8$ K (a) and 10 K (b) with the magnetic field applied along the indicated crystalline directions.

easy axis. When the magnetic field is applied along the [001] direction, M is linear with applied field up to 7 T with a magnitude much smaller than the saturation value for an applied field along the other directions, as expected for hard axis magnetization. At $T=10$ K, well above the transition temperature, M is linear to the field for low fields indicative of paramagnetic behavior and then approaches saturation values close to those at 1.8 K [shown in Fig. 2(b)].

Similar magnetic anisotropy has been reported in other rare earth single crystal compounds such as NdFe_2Si_2 ,¹⁶ CeNiGe_2 ,¹⁷ and $\text{Dy}_2\text{Ge}_2\text{O}_7$,¹⁸ and it has been attributed to strong anisotropy of crystal electric field that acts on the rare earth ions. Since Sc^{3+} is nonmagnetic, it is reasonable to expect that the magnetic anisotropy in DyScO_3 originates from the magnetocrystalline anisotropy of the Dy^{3+} ions.

In the main panel of Fig. 3 we plot the temperature dependence of the real part of the ac susceptibility $\chi'(T)$ of DyScO_3 as a function of temperature; the inset shows the corresponding imaginary part $\chi''(T)$. The magnitude of the applied ac field along [100] is 10 Oe over the frequency range from 10 Hz to 10 kHz. We observed two frequency-dependent maxima in $\chi'(T)$ in the measured temperature range, and maxima in $\chi''(T)$ corresponding to the sharp drops in the $\chi'(T)$ curves. The broad low temperature peak appears at 3.1 K and does not shift with frequency, consistent with expectations for a long-range magnetic transition. The observed decrease in the magnitude of $\chi'(T)$ with increasing frequency originates from the suppression of the high temperature peak at high frequency. The higher temperature maxima shift to higher temperature with increasing frequency, a feature which can be characteristic of a spin-glass transition. This possibility can be excluded, however, since there is no feature indicative of a phase transition in this temperature range in the dc measurements (see Fig. 1). Such a phenomenon has also been reported in canonical “spin ice”

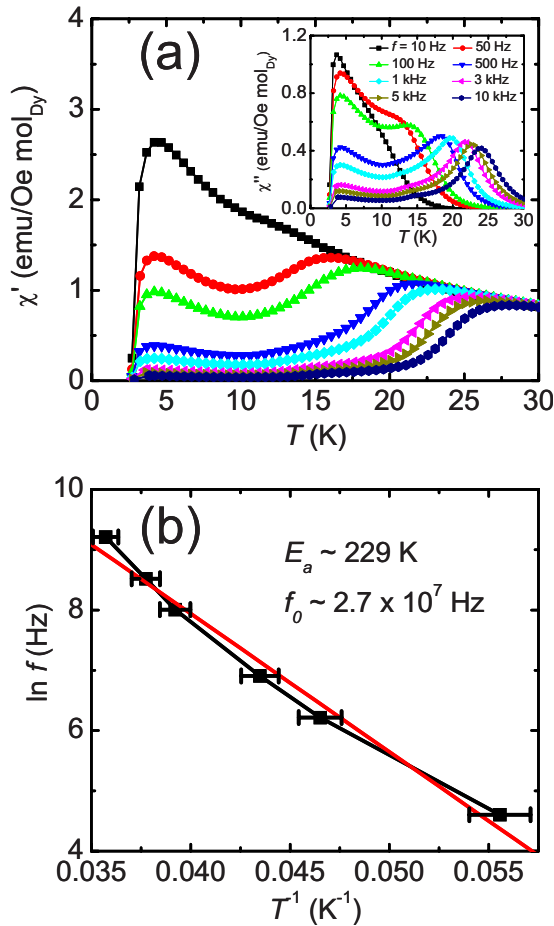


FIG. 3. (Color online) (a) The real part of the ac susceptibility, $\chi'(T)$, as a function of temperature at different frequencies with an ac magnetic field applied along the [100] direction. The inset shows the imaginary part, $\chi''(T)$. (b) The measurement frequency vs the inverse temperature at which the $\chi'(T)$ curves show high-temperature maxima. The error bars come from the temperature step size of 0.5 K used in this study. The red curve is an Arrhenius fit.

materials $\text{Dy}_2\text{Ti}_2\text{O}_7$,^{19,20} $\text{Dy}_2\text{Sn}_2\text{O}_7$,²¹ and $\text{Ho}_2\text{Ti}_2\text{O}_7$ (Ref. 22) and associated with the single ion anisotropy of the rare earth ions,^{20,22} which is consistent with the magnetocrystalline anisotropy observed in the magnetization data discussed above. Figure 3(b) shows the measurement frequency versus the inverse temperature at which the $\chi'(T)$ curves show maxima at high temperatures. The behavior can be fit well by an Arrhenius equation of the form $f=f_0e^{-E_A/k_B T}$ (see the red curve), where the activation temperature of E_A/k_B is about 229 K [similar to that of $\text{Dy}_2\text{Ti}_2\text{O}_7$ (Ref. 19)] and the attempt frequency f_0 is about 2.7×10^7 Hz. This strongly suggests that the high temperature spin freezing is a simple thermally activated relaxation process, and that the single-ion ground state is separated from the next lowest crystal field level by a spacing of around 200 K.

The phase transition we observe in DyScO_3 has important implications for its use as a substrate material. The anisotropy in the magnetization is sufficiently strong that samples physically secured by standard techniques physically crack or rotate when cryostat magnetic fields above a few tesla are applied. The antiferromagnetism of DyScO_3 also could have important implications for exchange biasing of ferromagnetic films grown on top of this substrate, and the total moment of the Dy ions in DyScO_3 is so large that the

transition masks the magnetic behavior of epitaxial films that are grown upon its surface, thus requiring optical techniques such as magneto-optical Kerr effect (MOKE) to probe the magnetism of such films. The combination of all of this behavior highlights a previously unrecognized concern for rare-earth perovskite substrates for the growth of novel strained materials. This is an important issue to be considered when the crystals serve as substrates for the epitaxial growth of thin films of magnetic oxides, as is increasingly the case as multiferroic films become of greater interest.

We gratefully acknowledge the financial support from the National Science Foundation through Grant No. DMR-0701582 and the MRSEC program (Grant No. DMR-0820404).

- ¹Landolt-Börnstein, *Numerical Data and Functional Relationships in Science and Technology*, edited by K. H. Hellwege and A. M. Hellwege (Springer, Berlin, 1976), New Series, Group III, Vol. 7e, pp. 11–13.
- ²D. G. Schlom, L. Q. Chen, C. B. Eom, K. M. Rabe, S. K. Streiffer, and J. M. Triscone, *Annu. Rev. Mater. Res.* **37**, 589 (2007).
- ³K. J. Choi, M. Biegalski, Y. L. Li, A. Sharan, J. Schubert, R. Uecker, P. Reiche, Y. B. Chen, X. Q. Pan, V. Gopalan, L. Q. Chen, D. G. Schlom, and C. B. Eom, *Science* **306**, 1005 (2004).
- ⁴J. H. Haeni, P. Irvin, W. Chang, R. Uecker, P. Reiche, Y. L. Li, S. Choudhury, W. Tian, M. E. Hawley, B. Craigo, A. K. Tagantsev, X. Q. Pan, S. K. Streiffer, L. Q. Chen, S. W. Kirchoefer, J. Levy, and D. G. Schlom, *Nature (London)* **430**, 758 (2004).
- ⁵A. Vailionis, W. Siemons, and G. Koster, *Appl. Phys. Lett.* **93**, 051909 (2008).
- ⁶T. Heeg, M. Roeckerath, J. Schubert, W. Zander, Ch. Buchal, H. Y. Chen, C. L. Jia, Y. Jia, C. Adamo, and D. G. Schlom, *Appl. Phys. Lett.* **90**, 192901 (2007).
- ⁷M. D. Biegalski, J. H. Haeni, S. Trolrier-McKinstry, and D. G. Schlom, *J. Mater. Res.* **20**, 952 (2005).
- ⁸R. Uecker, B. Veličkov, D. Klimm, R. Bertran, M. Bernhagen, M. Rabe, M. Albrecht, R. Fornari, and D. G. Schlom, *J. Cryst. Growth* **310**, 2649 (2008).
- ⁹V. V. Afanas'ev, A. Stesmans, C. Zhao, M. Caymax, T. Heeg, J. Schubert, Y. Jia, D. G. Schlom, and G. Lucovsky, *Appl. Phys. Lett.* **85**, 5917 (2004).
- ¹⁰H. M. Christen, G. E. Jellison, Jr., I. Ohkubo, S. Huang, M. E. Reeves, E. Cicerrella, J. L. Freeouf, Y. Jia, and D. G. Schlom, *Appl. Phys. Lett.* **88**, 262906 (2006).
- ¹¹C. Zhao, T. Witters, B. Brijs, H. Bender, O. Richard, M. Caymax, T. Heeg, J. Schubert, V. V. Afanas'ev, A. Stesmans, and D. G. Schlom, *Appl. Phys. Lett.* **86**, 132903 (2005).
- ¹²L. F. Edge, W. Tian, V. Vaithyanathan, T. Heeg, D. G. Schlom, D. O. Klenov, S. Stemmer, J. G. Wang, and M. J. Kim, *ECS Trans.* **16**, 213 (2008).
- ¹³R. M. Bozorth, H. J. Williams, and D. E. Walsh, *Phys. Rev.* **103**, 572 (1956).
- ¹⁴B. Veličkov, V. Kahlenberg, R. Bertram, and M. Bernhagen, *Z. Kristallogr.* **222**, 466 (2007).
- ¹⁵R. S. Roth, *J. Res. Natl. Bur. Stand.* **58**, 75 (1957).
- ¹⁶J. Vejpravová, P. Svoboda, V. Sechovský, M. Janeček, and T. Komatsubara, *Physica B* **328**, 173 (2003).
- ¹⁷A. P. Pikul, D. Kaczorowski, Z. Bukowski, T. Plackowski, and K. Gofryk, *J. Phys.: Condens. Matter* **16**, 6119 (2004).
- ¹⁸X. Ke, M. L. Dahlberg, E. Morosan, J. A. Fleitman, R. J. Cava, and P. Schiffer, *Phys. Rev. B* **78**, 104411 (2008).
- ¹⁹J. Snyder, J. S. Slusky, R. J. Cava, and P. Schiffer, *Nature (London)* **413**, 48 (2001); K. Matsuhira, Y. Hinatsu, and T. Sakakibara, *J. Phys.: Condens. Matter* **13**, L737 (2001).
- ²⁰J. Snyder, B. G. Ueland, A. Mizel, J. S. Slusky, H. Karunadasa, R. J. Cava, and P. Schiffer, *Phys. Rev. B* **70**, 184431 (2004).
- ²¹K. Matsuhira, Y. Hinatsu, K. Tenya, H. Amitsuka, and T. Sakakibara, *J. Phys. Soc. Jpn.* **71**, 1576 (2002); X. Ke, B. G. Ueland, D. V. West, M. L. Dahlberg, R. J. Cava, and P. Schiffer, *Phys. Rev. B* **76**, 214413 (2007).
- ²²G. Ehlers, A. L. Cornelius, M. Orendac, M. Kajnakova, T. Fennell, S. T. Bramwell, and J. S. Gardner, *J. Phys.: Condens. Matter* **15**, L9 (2003).